J. Astrophys. Astr. (1992) **13**, 217–239

Kinematics of the Cometary Globules in the Gum Nebula*

T. K. Sridharan *Raman Research Institute, Bangalore 560 080 and*
Joint Astronomy Program, Indian Institute of Science, Bangalore 560 012

Received 1992 April 21; accepted 1992 July 4

Abstract. We report a study of the kinematics of the cometary globules in the Gum Nebula using the $J = 1 \rightarrow 0$ transition line of ^{12}CO. A morphological center for the system with which 60% of the globules are associated is identified. It is shown that the observed radial velocities of the heads of the globules are consistent with an expansion of the system. Systematic velocity gradients are present along some of the tails. The estimated *expansion age* and the *tail stretching age* are both $\sim$ a few million years, suggesting a common origin for the expansion and the formation of the tails. The presence of young stars of similar ages in some of the globules points to star formation triggered by the same cause. Possible scenarios are briefly discussed.

Key words: Cometary globules—Gum Nebula—star formation

1. Introduction

It is now well established that many bright rimmed globules found in association with H II regions are sites of low mass star formation (Dibai 1963, Sugitani *et al.* 1989, Sugitani, Fukui and Ogura 1991, Cernicharo *et al.* 1991, Duvert *et al.* 1990). The earliest example of such star formation is the discovery of HH 46–47 in the cloud GDC 1 (ESO 210-6A) in the Gum Nebula discussed by Schwartz (1977) and Bok (1978). GDC 1 has characteristics similar to the Cometary Globules (CGs) found earlier by Hawarden & Brand (1976) and Sandqvist (1976) in the Gum-Vela region. Later, Zealey *et al.* (1983) and Reipurth (1983) found a total of 38 CGs in a survey of the SERC IIIa-J and ESO B plates of which 32 were in the Gum-Vela region. The Gum globules have the following characteristics:

- A compact dusty head.
- A long faintly-luminous tail extending from one side of the head; the other side has a sharp edge with narrow bright rims.
- The tails of these CGs point away from a general center.
- Sometimes the heads have embedded young stars in them.

It is now known that the CGs are not restricted to the Gum Nebula. The original list contains CGs in Orion and recently CGs have also been found in the Rosette Nebula

*In partial fulfillment of the requirements for the Degree of Doctor of Philosophy of the Indian Institute of Science.

(Block 1990). Carbon monoxide maps of molecular clouds in Orion show cometary structure with tails pointing away from the Ori OB1 Association (Bally *et al.* 1991). It is believed that the cometary globules are formed by the effects of UV radiation from young stars, stellar winds, and supernova shocks on nearby molecular clouds.

The globules in the Gum Nebula are in a complicated setting. This nebula is a large shell like structure (radius $\sim 18°$) seen in Hα (Gum 1952; 1955). The estimated distance of ~ 400 pc implies a radius of 125 pc (Brandt *et al.* 1971). In the general direction of the center of the nebula are the Vela SNR (age $\sim 10^4$ yrs), the Pup A SNR (age ~ 3700 yrs), ζ Pup (O4f), the most luminous star in the southern sky, the Wolf-Rayet binary γ^2 Vel (WC8 + O9), and a possible B Association. These objects together represent a significant source of ionising radiation and stellar wind. Various models have been proposed for the Gum Nebula in which some of these objects play an important role (see for example Bruhweiler, 1983). Whether the Gum Nebula is expanding or not has been a point of controversy in the past but latest studies indicate expansion (Srinivasan *et al.* 1987). In the central region of the Gum Nebula the CGs are distributed non-uniformly over a rough *annulus* whose center is close to the place from which the tails point away. This center is offset from the center of the Gum Nebula by about 4°. The best fit circle to the distribution of CGs has a radius of $\approx 9.5°$. There is firm evidence for star formation in some of the CGs as well as some of the other dark clouds in the Gum-Vela region (Schwartz 1977; Bok 1978; Reipurth 1983; Pettersson 1987, 1991; Graham 1986; Graham and Heyer 1989).

Soon after the discovery of HH 46–47, it was suggested that low mass star formation in the Gum Nebula may have been triggered by external events (Schwartz 1977), quite possibly the events responsible for the origin of the Gum Nebula itself (Brand *et al.* 1983). Stellar winds, SN shocks and shocks associated with the expansion of H II regions can compress small globules into gravitational instability leading to star formation. Numerical studies of such processes give credence to this idea (Woodward 1976; 1979). Reipurth (1983) has argued in favor of UV radiation from young stars being the cause for the origin of the CGs as well as star formation in them. There have also been studies of radiation driven implosion as a mechanism for star formation (Sandford, Whitaker & Klein 1982, Bertoldi & McKee 1990). Specifically Bertoldi & McKee (1990) have shown that clouds exposed to UV radiation will acquire a cometary structure.

The first systematic study of the CGs in the Gum Nebula was done by Zealey *et al.* (1983) (hereafter referred to as Z83). They made 4 cm formaldehyde absorption observations of 9 CGs with the Parkes 210 foot telescope. Only CGs big enough to have a good chance of detection with the 4.4′ beam were observed. Goss *et al.* (1980) had observed some of the CGs in an independent survey. Radial velocities for a total of 10 CGs were thus obtained. Z83 concluded from this data that the radial velocities were consistent with rotation of the system about an axis perpendicular to the galactic plane. They suggested that the orientation of this axis implied that the kinematics of the CGs is dominated by galactic rotation. In addition they found that in an l–v plot the CGs lined up on a straight line parallel to the HI data for the region, but offset in l. They took this to mean that the observed velocities of the CG complex are wholly due to large scale effects of the local spiral structure. Assuming that such a line represented galactic rotation effects they studied the deviations from the straight line fit to look for expansion or rotation. Their conclusion was that the CGs may be on a shell expanding up to 5 kms^{-1}. [We find this surprising since the residuals (i.e. the deviations from

their straight line fit) were only $\pm 2\,\mathrm{kms}^{-1}$]. In addition, from a study of the tails seen in optical photographs they identified two *centers* from where the maximum number of tails pointed away.

In this paper we wish to report ^{12}CO $J = 1 \rightarrow 0$ observations at 115.27 GHz of the system of cometary globules in the Gum Nebula using the 10.4 m millimeter-wave radio telescope at the Raman Research Institute, Bangalore (for a brief description of the telescope, see Patel 1990). The main objective was to make a more complete study of the kinematics of the system than was possible before. As was mentioned above, in previous attempts the velocity information was available only for 10 out of the more than 30 CGs. Since our beam size was 1′ we could detect even the smaller clouds that were not detected in the previous surveys. We also measured radial velocities along the tails of the CGs with a view to studying gas motions. The paper is organised as follows: In the next section the remeasured co-ordinates and the details pertaining to our observations are given. In section 3 we argue that there is a well defined *center* from where more than 60% of the tails point away. After a brief discussion of the distances to the CGs in section 4, in the following section we discuss the observed distribution of the radial velocities of the heads of the globules. In section 6 we show that these velocities are consistent with an expansion of the system from a common center with an expansion age of ~ 6 M yrs. The radial velocity measurements of the tails and their implications are given in section 7. The main results are discussed and summarised in section 8.

2. Observations

The CGs were observed in two separate runs in 1989 and 1990–91. The 1989 run using co-ordinates reported in literature detected only 18 out of the 29 CGs observed. Suspecting co-ordinate errors, the CG co-ordinates were remeasured from the ESO-SERC plates. The 1990–91 run using these new co-ordinates detected all the CGs except CGs 23 and 34. In addition to the heads, a few points along the tails were observed. An analysis of the statistics of detections and non-detections in the 1989 observations showed that the primary cause for non-detections during the 1989 run

Table 1. Co-ordinates of the Cometary Globules in the Gum Nebula.

	Co-ordinates (1950.0)												
	Head						Tail-end						
	RA			DEC			RA			DEC			Tail length (arc min)	Ref.
Source	h	m	s	°	′	″	h	m	s	°	′	″		
CG 01	7	17	49·7	−44	29	26.2	7	15	39.4	−44	29	2	23	M
CG 02	7	14	31.3	−43	52	43.8	7	12	49.3	−43	51	24.6	18	M
CG 03	7	37	45.9	−47	45	35.1	7	37	26	−47	47	51.4	4	M
CG 04	7	32	45.6	−46	50	8.9	7	30	40.5	−46	56	43.2	22	M
CG 05	7	39	15.8	−43	42	8.3	7	39	4.6	−43	41	55.1	2	M
CG 06	7	29	2.1	−46	37	14.5	7	28	18.9	−46	41	35	9	M

Table 1. Continued.

Source	Co-ordinates (1950.0) Head RA h	m	s	Head DEC °	′	″	Tail-end RA h	m	s	Tail-end DEC °	′	″	Tail length (arc min)	Ref.
CG 07	9	12	26.1	−42	16	54.4	9	13	14.2	−42	18	14.6	9	M
CG 08	7	41	1.3	−41	8	32.8	7	40	46.5	−41	8	23.2	3	M
CG 09	7	39	7.4	−41	20	4.4	7	38	52.6	−41	19	6.3	3	M
CG 10	7	40	55.2	−41	58	11.9	7	40	34.6	−41	59	48.4	4	M
CG 13	7	12	49.1	−48	23	16.4	7	10	17.6	−48	30	0.2	26	M
CG 14	7	37	16.2	−49	44	29.5	7	36	22.4	−49	52	51.8	12	M
CG 15	7	31	0.5	−50	39	20.2	7	29	55.2	−50	45	29.1	12	M
CG 16	7	26	19.4	−50	58	32.6	7	25	47	−51	1	48.7	6	M
CG 17	8	51	0	−51	41		8	51	6.5	−51	42	44.4	2	Z
CG 18	8	51	0	−50	29		8	51	2.6	−50	30	57.4	2	Z
CG 22 B1	8	26	48.0	−33	34	12.0	8	27	16.7	−33	14	12	21	S
CG 22 B2	8	27	16.7	−33	14	12.0	8	28	4.1	−32	46	11	30	S
CG 23	7	34	48	−50	6		7	34	14.6	−50	10	30	7	Z
CG 24	8	17	33.0	−42	44	58.4	8	17	14.5	−42	48	45.8	5	M
CG 25	7	35	56.0	−47	50	15.1	7	35	19.2	−47	54	47.5	8	M
CG 26	8	14	3.3	−33	40	52.8	8	14	12.9	−33	37	36.1	4	M
CG 27	8	10	28.4	−33	36	11.6	8	10	33	−33	33	53.6	2	M
CG 28	8	10	26.2	−33	46	32.4	8	10	25.8	−33	45	12	1	M
CG 29	8	10	27.9	−33	51	54.2	8	10	32.6	−33	49	36.1	3	M
CG 30	8	7	40	−35	56	2	8	7	13.4	−35	30	34.1	26	R
CG 31 A	8	7	10	−35	52	24	8	6	36.9	−35	26	53.2	26	R
CG 31 B	8	6	55	−35	54	14								R
CG 31 C	8	6	40	−35	50	44								R
CG 31 D	8	6	24	−35	52	58								R
CG 31 E	8	6	21	−35	55	18								R
CG 32 A	8	12	28.6	−34	21	8.4	8	12	10.8	−34	8	27.9	13	M
CG 32 B	8	12	22.4	−34	18	58.6	8	12	10.8	−34	8	27.9	11	M
CG 33	8	13	33.7	−33	55	19.4	8	13	40.3	−33	52	39	3	M
CG 34	7	27	54	−41	4		7	27	19	−40	57	24	9·4	Z
CG 36	8	35	22.7	−36	27	23.9	8	35	46.5	−36	22	47.1	7	M
CG 37	8	10	29.4	−32	56	21.7	8	10	30.8	−32	52	25.1	4	M
CG 38	8	7	47	−36	1	42								R
GDC 1	8	24	17	−50	52	5								R
GDC 2	8	25	10	−50	51	42								R
GDC 3	8	24	56	−50	41	13								R
GDC 4	8	25	2	−50	29	53								R
GDC 5	8	26	1	−51	0	2								R
GDC 6	8	30	30	−50	22	46								R
GDC 7	8	32	39	−50	8	21								R

References:
Z: Zealey *et al.*, 1983
R: Reipurth, 1983
S: Sahu *et al.*, 1988
M: Our measurements from ESO plates.
Notes:
1. For CGs 31 B, C, D, E and 38 tail co-ordinates are not available.
2. The Gum Dark Clouds (GDCs) have been included for completeness.

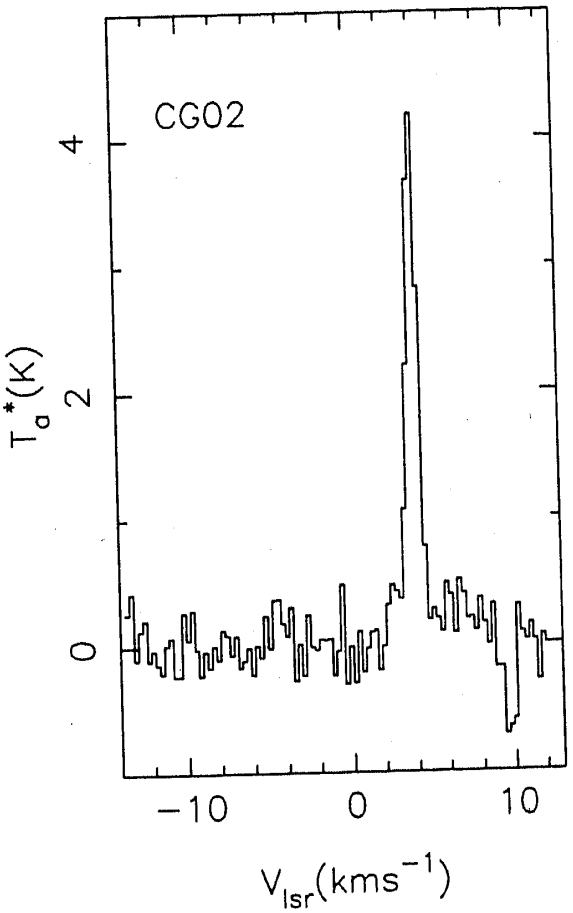

Figure 1. A sample spectrum from observations made during 1990–91. A fourth order polynomial has been subtracted to remove the baseline curvature due to frequency switching. The back-end was an AOS with 100 kHz resolution.

was the wrong co-ordinates used, combined with the small sizes of the heads of the CGs. The new measured co-ordinates of the heads and tail-ends along with the tail lengths are listed in Table 1.

Frequency switching by 15.25 MHz was used for all the observations. An ambient temperature chopper-wheel was used for calibration. The back-end was an acousto-optic spectrometer with 50 kHz resolution and 30 MHz coverage. The data was later bunched in frequency to get better S/N, giving spectra with 100 kHz resolution. Pointing was checked by beam switched continuum scans on Jupiter (See Patel 1990 for details). Fourth order polynomials were fitted to remove baseline curvature. A sample spectrum is shown in Fig. 1. Table 2 lists the noise levels, measured antenna temperatures and the LSR velocities found by fitting gaussians to the lines from the heads of the CGs.

3. The center of the distribution of the CGs

For any assumed center, the tail position angle θ_{TH} with respect to the line joining the head and the center can be calculated using spherical geometry. The center and the head of a CG can be joined by a great circle on the celestial sphere. The tail forms a part

Table 2. 1990–91 observations.

Source	T_a^* K	v_{LSR} kms^{-1}	v_{FWHM} kms^{-1}	rms K
CG 01	5.3	3.3	1.4	0.33
CG 02	4.2	4.1	0.9	0.22
GC 03	3.3	0.1	1	0.32
CG 04	1.2	1.7	1.2	0.25
CG 06	2.9	0.9	1.1	0.26
GC 07	5.2	−1.1	0.6	0.54
GC 08	1.7	−5.8	1	0.2
GC 09	3.9	−4.2	1.3	0.59
CG 10	3.9	−5.5	1.0	0.19
CG 13	3.7	3.7	0.8	0.41
GC 14	3.0	−0.9	1	0.28
CG 15	3.6	−0.8	0.6	0.57
CG 16	2.9	−0.7	0.7	0.22
CG 17	0.8	3.7	0.8	0.33
CG 18	1.0	2.0	0.4	0.26
CG 22 B1	6.4	6.5	1.1	0.41
CG 22 B2	6.8	6.8	1.3	0.28
CG 22 B3	3.4	6.4	1.4	0.22
CG 24	2.9	−12.5	1.2	0.2
CG 25	2.2	−1.8	0.8	0.29
CG 26	3.5	2.0	1	0.51
CG 27	2.8	5.0	0.8	0.44
CG 28	2.9	5.2	1.1	0.54
CG 29	2.4	5.2	0.7	0.31
CG 30	3.8	5.8	2.2	0.25
CG 31 A	4.5	6.0	1.3	0.44
CG 31 B	4.2	6.0	1	0.36
CG 31 C	6.8	6.3	1.6	0.3
CG 31 D	1.5	6.9	1.6	0.29
CG 32 A	4.5	4.9	1.2	0.43
CG 32 B	4.7	4.8	1	0.38
CG 33	2.3	1.6	0.6	0.46
CG 36	1.4	−8.5	0.7	0.39
CG 37	3.0	6.2	0.4	0.48
CG 38	1.7	7.0	1.2	0.23
GDC 1	5.6	5.3	1.3	0.36
GDC 2	5.1	6.0	1.4	0.36
GDC 3	1.9	5.9	1.0	0.43
GDC 4	3.1	4.9	1.3	0.52

of another great circle. θ_{TH} is angle between these two great circles. To identify a center for the system of CGs we associate with every point in the central region a fraction f, defined as the fraction of CGs with θ_{TH} (calculated using that point as the center) within $\pm 10°$. We evaluated f over a $15° \times 15°$ area in the central region with grid points separated 0.5° in both α and δ. Figure 2 shows a contour plot of f. Only those CGs have been used for which we have measured the co-ordinates. CG 24 has not been included because of its anomalous tail direction. The CGs used in the analysis are shown as filled circles with tails and the unused CGs are shown as open circles with tails. For clarity the tail lengths shown have been scaled up 10 times. The contour spacing is 0.05 with

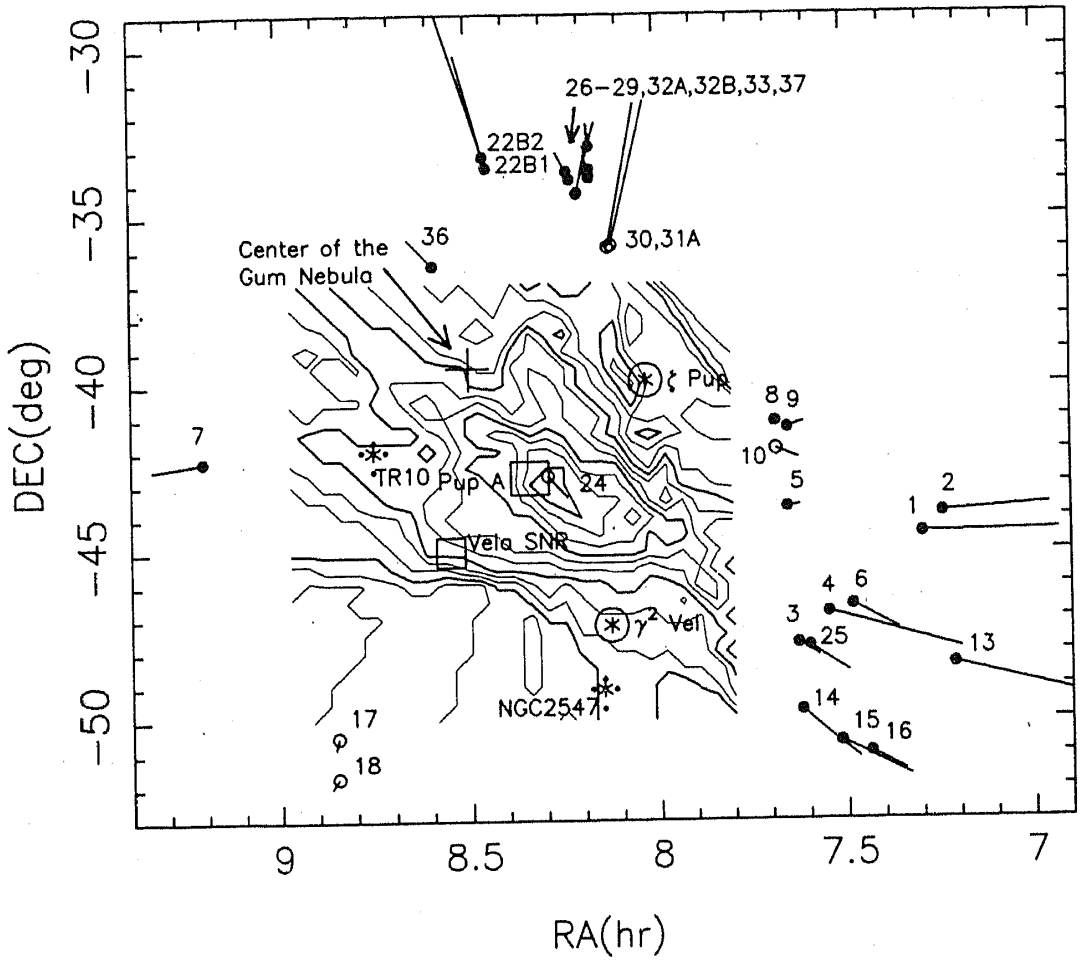

Figure 2. The figure shows contours of constant f where f is the fraction of the cometary globules with position angles of their tails $\leqslant 10°$. The position angles are measured with respect to the line joining the head of the globule and any particular point in the region. The inner most contour bounds the region where for at least 60% of the globules the position angles of the tails are $\leqslant 10°$. The contours are drawn in steps of 0.05 in f and were evaluated with a grid spacing of $0.5° \times 0.5°$. Every third contour is shown as a thick line. We designate the central maximum as the morphological center of the system. The globules used for evaluating the contours are shown as filled circles with tails and those not used as open circles with tails. For clarity, the tails have been scaled up 10 times. In addition the figure shows several other interesting objects such as the Pup A SNR, the Vela SNR, ζ Pup, γ^2 Vel and the open clusters TR 10 and NGC 2547.

every third contour drawn as a solid line. One can see that there is a central maximum with which 60% of the CGs are associated. The locations of the various interesting objects such as ζ Pup, γ^2 Vel, the Vela SNR etc. are marked in the figure. There are no strong local maxima associated with any of these objects. This indicates that most of the CGs are affected by a combination of objects rather than a particular object. The co-ordinates of the central maximum are $\alpha = 8^h 17^m$ and $\delta = -43°$. We will refer to this point as the *center* hereafter. The *center* deduced by us is 1.5° north of *center1* of Z83. Reducing the limiting θ_{TH} from $\pm 10°$ to $\pm 5°$ for calculating f merely results in increased noise on the contour plot. The apparently anomalous CG 24 tail can be understood by noticing that it is so close to *center* that even small errors in the location of *center* can make the tail direction look anomalous.

In view of the remarkable near coincidence of the deduced *center* with the SNR Pup A it is worth briefly discussing whether the two may be causally connected. Zarnecki *et al.* (1978) estimate a distance of 1 kpc for Pup A from X-ray absorption measurements. The $\Sigma - D$ distance to Pup A is $2 - 2.5$ kpc (Milne 1979, Casewell & Lerche 1979) although it should be emphasised that this method has been severely criticised in the literature (Srinivasan & Dwarakanath 1982; Green 1984). The latest estimate based on the kinematic distance to molecular clouds interacting wih Pup A gives 2.2 kpc (Dubner & Arnal 1988). We will therefore adopt a distance of 2 kpc to Pup A. At this distance it would be very difficult to detect the CGs, especially the ones close to the galactic plane. If the CGs are placed at the estimated distance to Pup A, then they will be ≈ 200 pc away from the SNR. From the size of the SNR it is clear that the SN shock has not reached the CGs. So the only way Pup A may be associated with the formation of the CGs is through the photon pulse at the time of the explosion or alternatively the UV radiation and stellar wind from its *progenitor*. The age of Pup A has been estimated to be ~ 3700 yrs (Winkler *et al.* 1988). From the measured electron density of $\sim 100\,\mathrm{cm}^{-3}$ for the bright rim of CG30 (Pettersson 1984) we estimate a recombination lifetime $t_{\mathrm{recomb}} = (n_e \alpha)^{-1} \sim 1200$ years. So it is difficult to see how the presently observed bright rims can be due to the initial excitation by the supernova flash. There is a further argument. Both the expansion age of the system of CGs and the age of the tails estimated in later sections are $\sim$ a few million years, thus making a causal association between Pup A and the CGs very unlikely. We therefore conclude

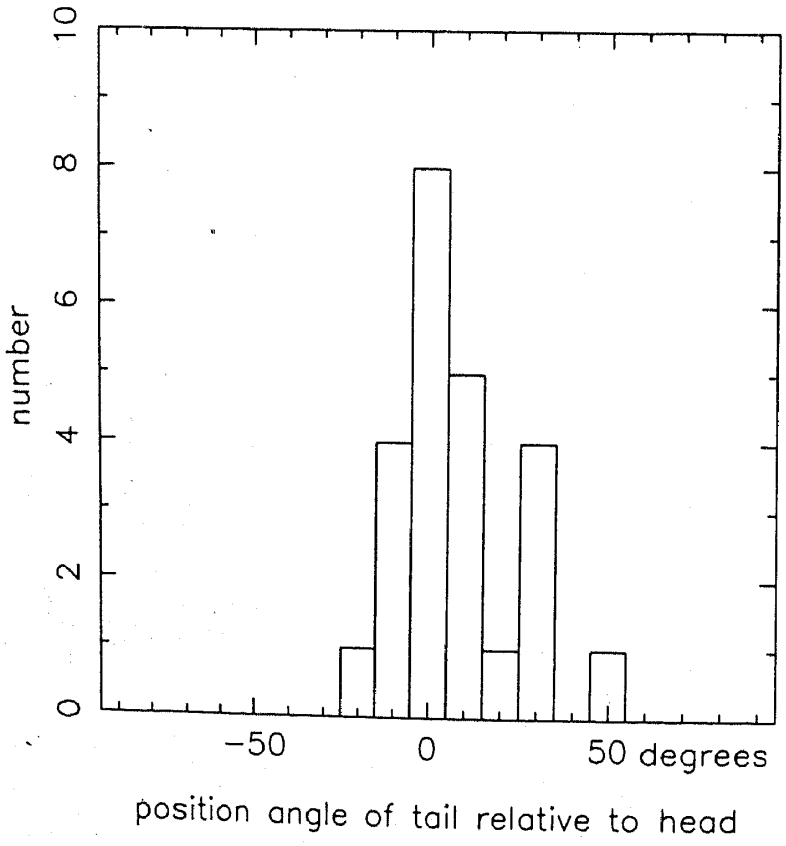

Figure 3. The distribution of the position angles θ_{TH} of the tails relative to the line joining the *center* and the respective heads for 24 CGs.

that the coincidence of Pup A and the *center* is a chance superposition. On similar grounds we rule out any role for Vela SNR in the formation of the CGs.

Figure 3 shows the distribution of θ_{TH}. We see that apart from the central peak there is a peak at 35° consisting of four globules, viz. CGs 26, 27, 29 and 33. Although the peak is not statistically significant, the directions of their tails suggest that they may be associated with ζ Pup alone. It is possible that they are closer to ζ Pup in the direction perpendicular to the plane of the sky. Even though we cannot associate a single object of any importance with the *center*, we will use it as the center of the distribution of the CGs for further analysis. The other objects in Fig. 2 are discussed in the next section.

4. Distance to the CGs

The most important objects in the region of the CGs from the point of view of momentum and energy are ζ Pup, γ^2 Vel, and the clusters NGC 2547 and TR 10. All these objects are at a distance of $\sim$ 450 pc (Eggen 1980; Claria 1982). As seen in Fig. 4, a histogram of the distances of the early type stars towards the Gum Nebula used by Wallerstein, Silk & Jenkins (1980) to study gas in the nebula shows a peak at 450 pc. In an earlier study of the Gum Nebula, Brandt *et al.* (1971) had identified a possible B Association at 450 pc distance which has been later named Vela OB2. So it is clear that at a distance of 450 pc there exists a significant population of early type stars. The

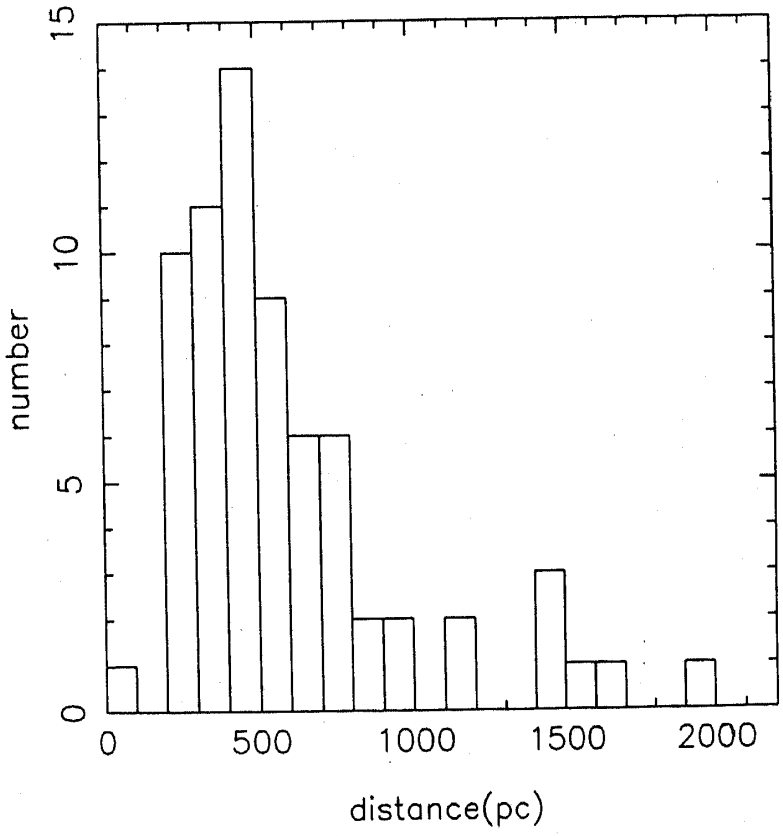

Figure 4. The distribution of the distances to the early type stars towards the Gum Nebula. The distances are from Wallerstein, Silk & Jenkins (1980).

location of some of these objects are shown in Fig. 2. The point to note is that these objects, some of which have to be necessarily invoked to explain the CGs, are at about the same distance and are centrally located with respect to the distribution of the CGs. So we assume that the CGs are at the same distance as these objects, viz. at ~ 450 pc. Further, Pettersson (1987) has estimated a lower limit for the distance to CG 30–31 complex to be 420 pc using a foreground star, and the distance to the young star in the head of CG 1 has been estimated to be ~ 500 pc (Brand *et al.* 1983). Adopting a distance of 450 pc would imply that the distribution of the CGs extends to about 150 pc perpendicular to the line of sight.

5. Radial velocities

From the observations described in section 2, we have radial velocities for all the CGs except CG 23 and CG 34 which were not detected. The radial velocities were obtained as the center velocity of the best fitting gaussian to the lines. As CG 10 and CG 30 show two components, we take the velocity of the stronger component.

The Columbia CO survey of the third galactic quadrant (May *et al.* 1988) covered a part of the region over which the CGs are distributed. Since this survey was done at 0.5° resolution we do not expect to see the small CGs because of beam dilution. But any larger scale distribution of CO along lines of sight to the CGs will show up. We can use these to check if our detections are contaminated by molecular gas not associated with the CGs. We see from the published survey data that CGs 1–6, 8–10, 13–16 and 25 are outside the region covered in the survey. This therefore leaves one with some uncertainty. But the CGs 1–4, 6, 13–16 and 25 have $b < -12$ and so their detections are unlikely to be confused by more widespread gas. CGs 5, 8, 9 and 10 have $b \sim -9$ and have nearby dark clouds distributed over larger spatial scales. These dark clouds show signs of being affected by ζ Pup and γ^2 Vel. These four CGs show more or less the same radial velocities. All the other CGs are in a region covered by the survey. The GDC complex of which GDCs 1 and 2 show CG features is extended consisting of 7 clouds and has been detected by the survey. The velocities are consistent. Similarly the CG 30–31 complex, which is extended with more dark clouds in the same region, and the largest globule CG 22, have been detected by the survey with velocities consistent with our values. All other CGs which are small and isolated have not been detected. So it is clear that the radial velocities we have obtained are reliable and do not suffer from contamination from other line-of-sight material. In addition, the fact that the 1989 observations using co-ordinates with errors resulted in a lower detection rate supports this conclusion. The survey detected strong CO emission from what is called the Vela Molecular Ridge (VMR), but it has been shown that this emission arises from GMCs at distances 800–2400 pc (Murphy 1985).

A comparison of our velocities with those of Z83 shows general agreement except for CG17, for which we measure a velocity of $+3.7\,\mathrm{kms}^{-1}$ as against the value of $-6.5\,\mathrm{kms}^{-1}$ due to Z83. The radial velocity we measure for CG 18 ($\approx 1°$ away from CG 17) is $+2.0\,\mathrm{kms}^{-1}$. The velocities of the clouds in the GDC 1–7 complex which is nearby are again in the range $+5$ to $+6\,\mathrm{kms}^{-1}$. GDC 1 and GDC 2 have a windswept appearance with tail-like structures pointing in the same general direction as the other CGs and bright rims facing the center. The rough agreement between the velocities of CG 17, CG 18 and the GDCs suggests that the value reported by Z83 for CG 17 may be

in error. As they have not published their spectra, nor mentioned their S/N, we are not in a position to comment any further.

We now wish to discuss the implications of these radial velocities. First, we briefly touch upon the suggestion made by Z83, viz. that the velocity distribution can be understood in terms of the large scale galactic rotation effects. In Fig. 5 we have plotted the radial velocities against the position angles of the CGs measured with respect to the *center* with zero towards north and increasing through east. The sinusoid fitted by Z83 which led them to suggest a rotation of the system of CGs is also shown. Clearly, the fit is very poor. There are two reasons why the sinusoid is a poor fit to the new data: (i) the revised value of the radial velocity of CG 17, and (ii) velocities of the CGs not detected earlier. Our main conclusion from this figure is that the model of the system of CGs rotating about an axis perpendicular to the galactic plane is untenable. In Fig. 6 we have plotted the radial velocities against galactic longitude. Again, the new data does not permit a simple straight line fit as suggested earlier (Z83), and therefore an explanation based on galactic rotation effects is hard to reconcile. Nevertheless, the contribution due to galactic differential rotation will be present and should be removed before attempting to interpret the velocities.

Before one can correct for the galactic differential rotation one must assume a mean distance to the CGs. Based on the discussion given in section 4, we will adopt a distance of 450 pc. The dashed line in Fig. 6 represents the expected radial velocities for different

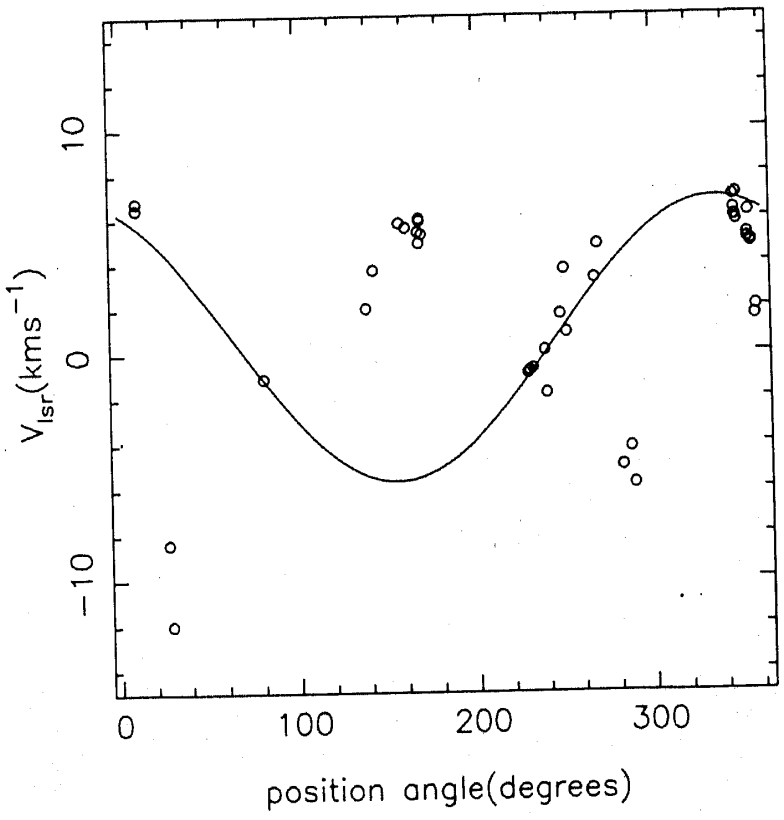

Figure 5. The velocities of the globules in the Gum Nebula with respect to the Local Standard of Rest. The horizontal axis is the position angle of the globules: zero is north and the position angle increases through east. The sinusoid shown is the fit made by Zealey *et al.* (1983) for their data.

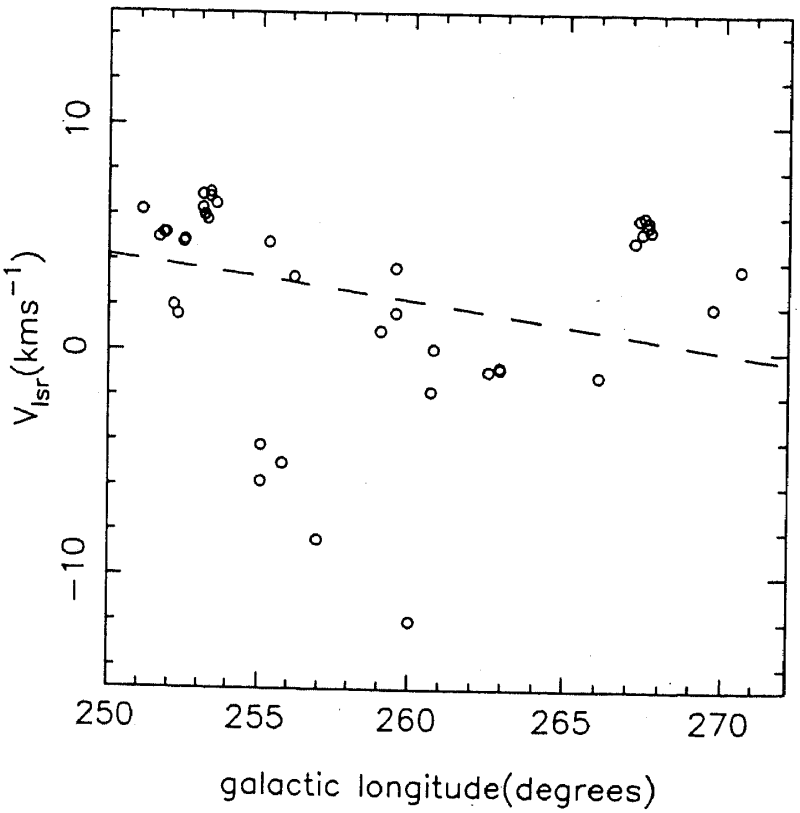

Figure 6. The velocities of the globules in the Gum Nebula with respect to the Local Standard of Rest versus the galactic longitude. The broken line shows expected velocities due to galactic differential rotation for an assumed heliocentric distance of 450 pc and $b = 0$.

galactic longitudes from the well known formula

$$v_r = Ar \sin(2l) \cos^2 b \tag{1}$$

with the heliocentric distance $r = 450$ pc and $b = 0$. We have assumed a value of 14.5 $kms^{-1} kpc^{-1}$ for Oort's constant A(Kerr & Lynden-Bell 1986). The significant deviations of the observed radial velocities from the expected value given by the dashed line suggests local motions in the system of CGs. Fig. 7 shows the residuals after galactic rotation effects have been subtracted out using Equation 1. It should be remarked that the differences in the line-of-sight distances to the various globules (~ 150 pc) can only account for a scatter of ~ 1.4 kms^{-1}.

6. Expansion of the globules

In this section we wish to argue that the velocity residuals can be easily understood in terms of an expansion of the system of globules from a common center. If the CGs are distributed over a shell expanding with uniform velocity then, as can be seen from Fig. 8(a) the expected velocities are given by

$$v_{rad} = \pm v_{exp}(1 - \sin^2 \theta / \sin^2 \theta_{max})^{1/2} \tag{2}$$

where v_{exp} is the expansion velocity of the shell, v_{rad} is its line-of-sight component, and θ_{max} is the angular distance of the farthest CG from the *center*. In this case one would

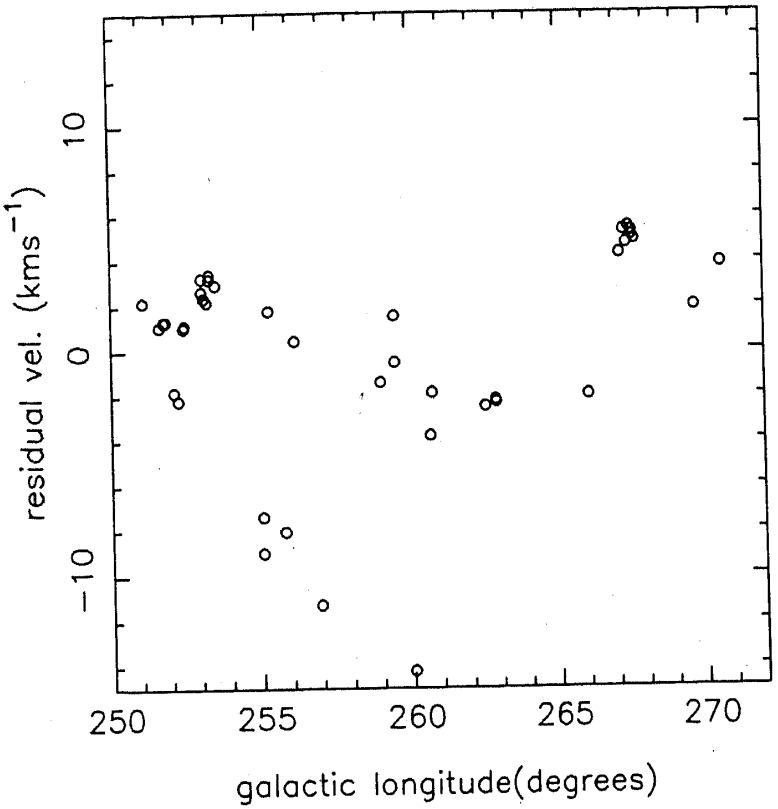

Figure 7. The residual velocities of the globules in the Gum Nebula after removing the contribution of the galactic differential rotation. A mean distance of 450 pc to the globules has been assumed.

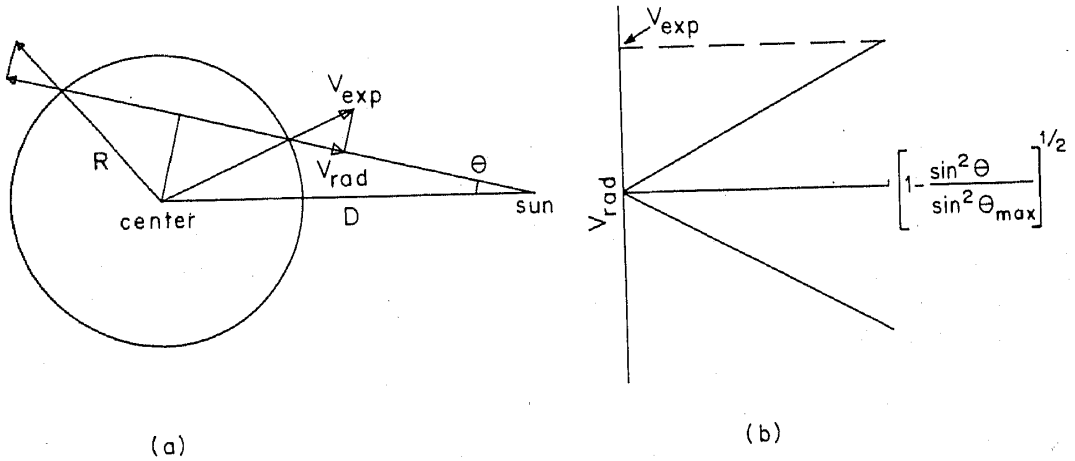

Figure 8. (a) Schematic diagram for deriving expected velocities from an expanding shell of objects. V_{exp} is the expansion velocity whose radial component is V_{rad} and θ is the angular distance to any point on the shell from the center of the shell. (b) The expected velocity plotted against $(1-\sin^2\theta/\sin^2\theta_{max})^{1/2}$.

expect the residual velocities, when plotted against $(1-\sin^2\theta/\sin^2\theta_{max})^{1/2}$, to fall on two straight lines as shown in Fig. 8(b). If the CGs are not on a shell but distributed throughout the sphere, then the region between the lines will be filled up provided the inner CGs move slower than the outer CGs. If the distribution of the CGs within the sphere is not uniform one will find an incomplete filling of this region.

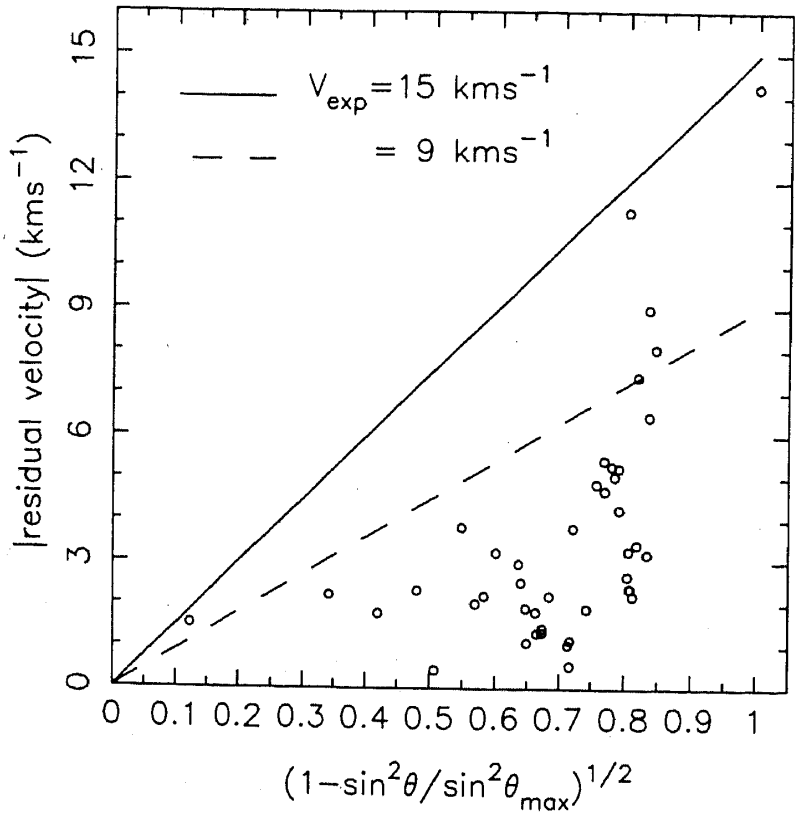

Figure 9. The absolute values of the residual velocities of the globules plotted against $(1-\sin^2\theta/\sin^2\theta_{max})^{1/2}$ where θ is the angular distance to the globule from the *center*. The line shown corresponds to a shell expanding at 12 kms^{-1}.

Figure 9 shows the absolute value of the residual velocities plotted against $(1-\sin^2\theta/\sin^2\theta_{max})^{1/2}$ for all the CGs and the GDCs. We have taken θ_{max} to be 12.5°, corresponding to CG 13. It is clear that there is an upper limit to the velocities which increases as one goes closer to the center (abscissa = 1) implying an expansion of the system. A contraction of the system will also have the same signature, but is very unlikely. The two straight lines shown correspond to expansion velocities of 15 kms^{-1} and 9 kms^{-1}. We will adopt an expansion velocity of 12 kms^{-1}. The figure further shows that the CGs are distributed over a volume rather than in a shell, and that the distribution is not uniform. Finally, the inferred expansion velocity of 12 kms^{-1} implies an *expansion age* of $\sim$6 M yrs.

7. Radial velocities along the tails

In addition to measuring the radial velocities of the heads of the cometary globules, we also measured the velocities along the tails. In this section we discuss these observations. The results of the observations of the tails are listed in Table 3. The velocities were obtained by fitting gaussians to the lines. We estimate the error on the velocities to be 0.15 kms^{-1} from several observations of the head of CG 22 spread over two months. We will regard this rms as the error on all radial velocity measurements.

Out of 21 CGs for which at least three points along the tails were observed, seven

Table 3. Observations of the tails.

Source	T_a^* K	v_{LSR} kms^{-1}	v_{FWHM} kms^{-1}	rms K	Distance from head in arcmin	Velocity gradient kms^{-1} arcmin^{-1}
CG 1 H	5.3	3.3	1.4	0.33	0.0	0.019
CG 1 T 2	4.0	3.7	1.1	0.55	14.2	(±0.003)
CG 1 T 3	4.2	3.7	1.4	0.39	21.2	
CG 1 T 4	4.3	3.4	1.4	0.43	7.0	
CG 2 H	4.2	4.1	0.9	0.24	0.0	0.040
CG 2 T 1	1.0	5.1	0.6	0.19	25.3	(±0.004)
CG 2 T 3	1.5	4.9	0.9	0.28	19.1	
CG 2 T 4	3.4	4.5	1.4	0.41	6.5	
CG 3 H	3.3	0.0	0.9	0.33	0.0	−0.014
CG 3 T 2	2.0	0.1	0.9	0.32	2.1	(±0.068)
CG 3 T 3	2.6	0.1	0.8	0.37	3.2	
CG 3 T 4	4.3	0.3	1.1	0.36	1.0	
CG 4 H	1.2	1.7	1.2	0.23	0.0	0.016
CG 4 T 1	4.9	1.9	1.2	0.49	17.4	(±0.021)
CG 4 T 2	5.6	1.3	1.5	0.43	8.7	
CG 4 T 3	5.3	1.7	1.3	0.50	13.0	
CG 6 H	2.9	0.9	1.1	0.26	0.0	0.061
CG 6 T 1	1.7	1.6	1.5	0.22	10.9	(±0.032)
CG 6 T 2	1.5	0.8	0.8	0.20	5.4	
CG 6 T 3	1.0	0.9	1.1	0.21	8.1	
CG 6 T 4	3.5	0.8	1.0	0.35	2.7	
CG 7 H	5.4	−1.1	0.6	0.54	0.0	−0.133
CG 7 T 2	4.1	−1.3	0.7	0.51	1.0	(±0.038)
CG 7 T 3	2.4	−1.3	0.9	0.43	1.4	
CG 7 T 4	5.4	−1.2	0.8	0.25	0.5	
CG 9 H	2.7	−4.1	1.1	0.20	0.0	0.080
CG 9 T 2	4.1	−4.1	1.0	0.45	1.6	(±0.09)
CG 9 T 3	3.3	−3.8	1.1	0.32	2.5	
CG 9 T 4	3.5	−3.9	1.1	0.32	0.9	
CG 10 T 2	5.8	−4.7	2.0	0.48	1.4	−0.056
CG 10 T 3	5.9	−4.5	1.9	0.36	2.0	(±0.25)
CG 10 T 4	4.4	−4.4	2.0	0.33	0.7	
CG 14 H	3.0	−0.8	1.0	0.28	0.0	−0.018
GC 14 T 2	1.5	−0.9	1.0	0.44	7.4	(±0.005)
CG 14 T 3	4.6	−1.0	0.7	1.37	11.3	
CG 15 H	3.6	−0.8	0.5	0.58	0.0	−0.005
CG 15 T 2	3.6	−0.8	0.8	0.52	8.1	(±0.018)
CG 15 T 4	3.8	−0.7	0.9	0.34	4.0	
CG 16 H	3.1	−0.7	0.8	0.20	0.0	−0.018
CG 16 T 1	1.3	−0.8	1.0	0.17	6.6	(±0.013)
CG 16 T 2	3.9	−0.7	1.1	0.53	3.4	
CG 16 T 3	2.7	−0.8	1.0	0.52	5.0	
CG 24 H	2.9	−12.4	1.14	0.19	0.0	−0.024
CG 24 T 1	0.3	−12.4	2.14	0.15	4.2	(±0.089)
CG 24 T 2	0.6	−12.0	2.00	0.21	2.1	
CG 24 T 4	2.9	−12.0	1.20	0.44	1.0	

Table 3. Continued.

Source	T_a^* K	v_{LSR} kms^{-1}	v_{FWHM} kms^{-1}	rms K	Distance from head in arcmin	Velocity gradient kms^{-1} arcmin^{-1}
CG 26 H	2.5	2.1	0.9	0.18	0.0	0.010
CG 26 T 1	1.7	2.2	1.0	0.24	3.5	(±0.02)
CG 26 T 3	2.3	2.2	0.9	0.18	2.6	
CG 26 T 4	4.6	2.2	0.9	0.41	0.9	
CG 27 H	2.0	5.2	0.7	0.25	0.0	0.021
CG 27 T 2	4.2	5.1	0.7	0.40	1.2	(±0.052)
CG 27 T 3	2.5	5.2	0.8	0.37	1.8	
CG 27 T 4	2.5	5.1	0.8	0.29	0.6	
CG 29 H	2.4	5.2	0.7	0.30	0.0	0.041
CG 29 T 1	2.6	5.3	0.7	0.24	2.5	(±0.02)
CG 29 T 3	1.7	5.2	0.8	0.18	1.9	
CG 31 A	4.5	6.0	1.3	0.42	0.0	0.036
CG 31 AT 1	1.7	6.9	1.9	0.22	25.3	(±0.006)
CG 31 AT 2	3.8	6.3	1.9	0.15	12.6	
CG 31 AT 3	3.5	6.6	1.8	0.14	19.0	
CG 32 AT 2	2.5	5.2	1.2	0.39	7.7	0.057
CG 32 AT 3	4.9	5.5	1.4	0.35	10.5	(±0.007)
CG 32 AT 4	6.6	5.0	1.0	0.36	3.8	
CG 32 AH	4.5	4.9	1.2	0.43	0.0	
CG 32 BH	4.7	4.8	1.0	0.38	0.0	0.114
CG 32 BT 2	3.8	5.4	1.0	0.41	5.5	(±0.043)
CG 32 BT 4	3.0	4.8	1.4	0.41	2.7	
CG 33 H	2.4	1.6	0.5	0.45	0.0	0.082
CG 33 T 1	1.6	1.9	0.5	0.35	3.0	(±0.032)
CG 33 T 2	3.1	1.8	0.7	0.43	1.6	
CG 33 T 3	2.0	1.8	0.6	0.24	2.2	
CG 33 T 4	2.3	1.8	0.5	0.51	0.7	
CG 36 H	3.1	10.4	0.7	0.35	0.0	0.144
CG 36 T 2	2.8	10.7	0.9	0.35	2.4	(±0.05)
CG 36 T 4	4.2	10.6	1.1	0.40	1.2	
CG 37 H	3.0	6.7	0.4	0.46	0.0	0.017
CG 37 T 3	1.0	6.8	0.6	0.22	2.9	(±0.064)
CG 37 T 4	2.0	6.9	0.8	0.20	1.0	

Note: CG 33 H, for example, refers to the head of the globule CG 33. Similarly, T refers to the tail. T4, T2, T3, T1 represent the sequence of points along the tails moving away from the head. The numbers in parenthesis are estimated errors in the velocity gradients (see text).

show very pronounced and systematic velocity shifts. In Fig. 10 the measured velocities are plotted against the distance from the head for some of these. The velocity gradients Δv_m in kms^{-1} arcmin^{-1} were obtained by fitting straight lines which are also shown in the figure. These gradients are also listed in Table 3, along with the estimated errors in the gradients. In Fig. 11 the velocity difference between the head and the extreme end of

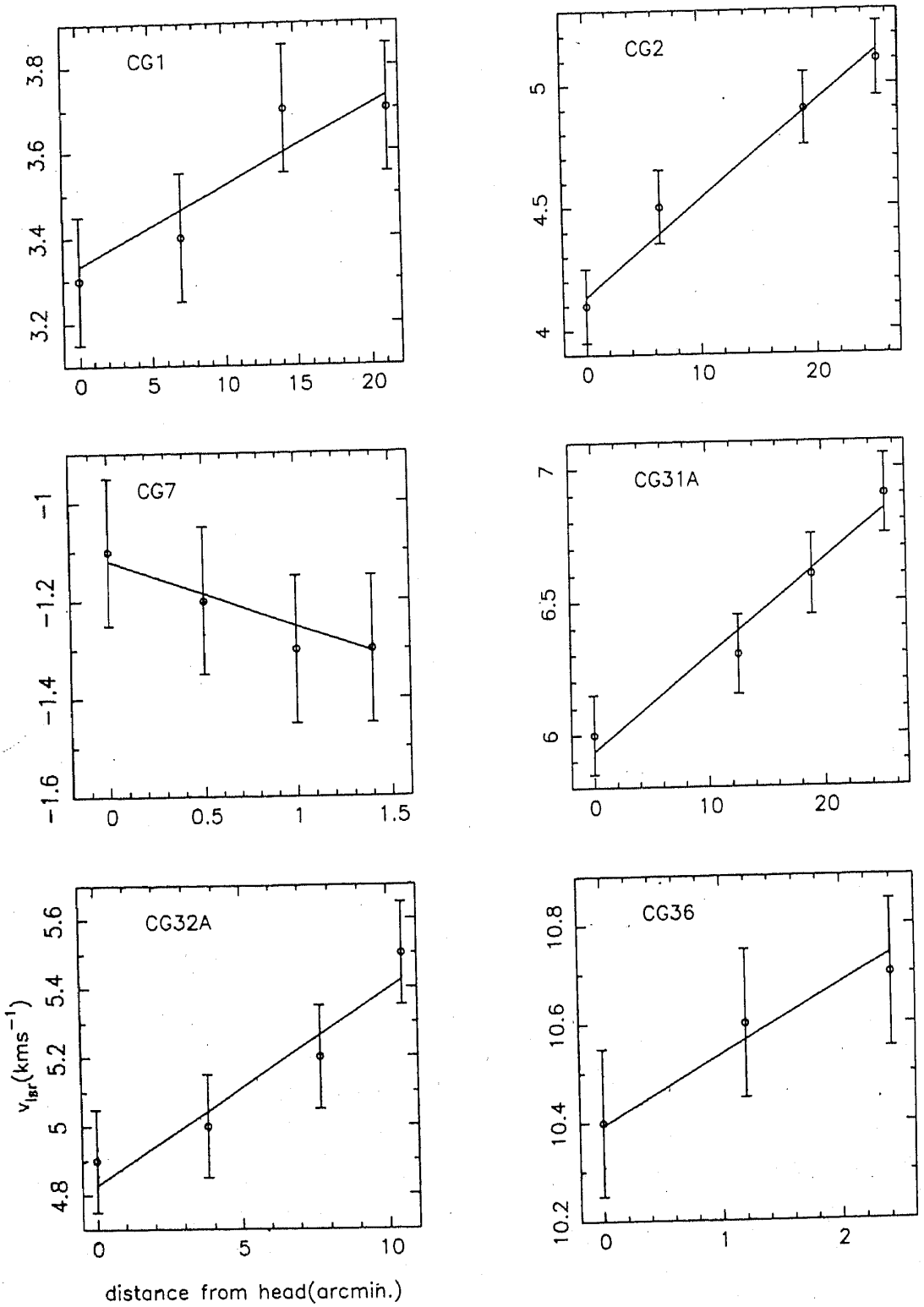

Figure 10. The velocity gradients along the tails for 6 out of 7 CGs which show pronounced gradients. The straight lines are least square fits to the data points.

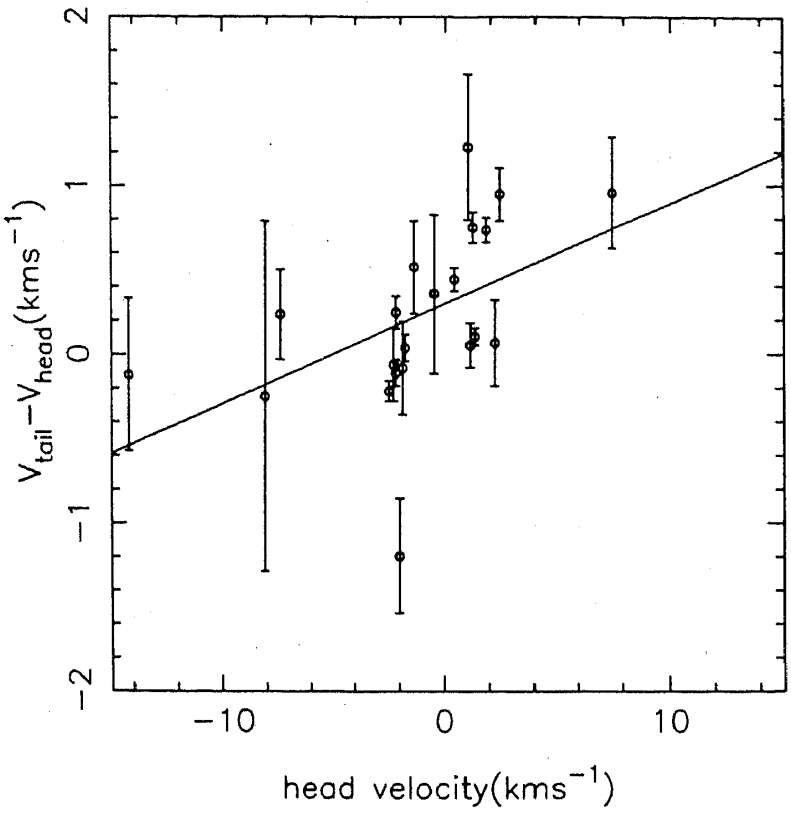

Figure 11. The difference in velocities between the ends of the *tails* and the respective *heads* plotted against velocities of the heads of the CGs.

the tail is plotted against the velocity of the head for all the 21 CGs. More precisely, the ordinate is calculated as the product of the velocity gradient along the tail and the tail length. The velocity differences so calculated are affected less by errors in the individual measurements. As may be seen, the data points fall approximately on a straight line passing close to the origin. This implies that the gas at the ends of the tails is moving faster than the heads and in the same direction as the heads.

If we assume that the tails are formed due to the stretching effect of these velocity differences over the course of time, one can calculate an age for the tails as the time taken for the presently observed velocity difference to result in an elongation equal to the measured tail length. Since we have only the *radial* component for the velocity differences and the *transverse* component of the tail lengths, the calculated ages suffer from projection effects. Figure 12 shows the distribution of the estimated apparent ages of the tails in millions of years; a distance of 450 pc has been assumed. The apparent age is related to the real age through the relation

$$t_{\text{apparent}} = t_{\text{real}} \times \tan\theta \tag{3}$$

where θ is the angle between the tail and the line of sight. Since most of the CGs are towards the periphery we believe that most CGs have $\theta > 45°$. So the apparent age represents an over estimate of the real age. We feel that ~ 3 M yrs is a reasonable estimate for the ages of the tails.

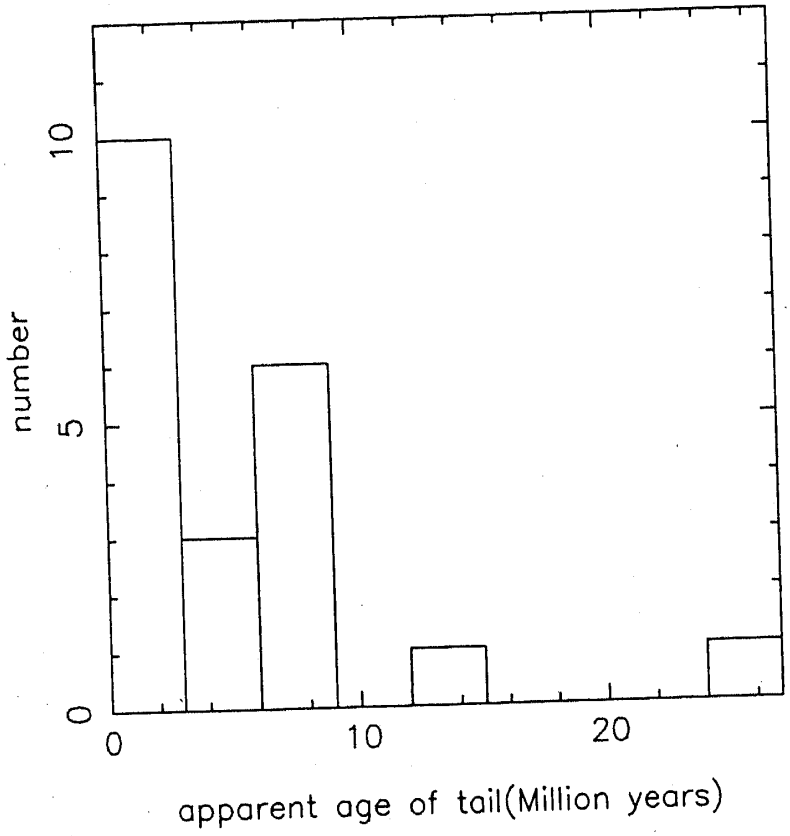

Figure 12. A histogram of the apparent *tail stretching ages* defined as the time required for the velocity difference between the heads and the tail-ends of the CGs to stretch the globules to their observed lengths.

8. Discussion and summary

The main results obtained in the previous two sections are the following:

(i) The system of cometary globules in the Gum Nebula appears to be expanding from a common center. The *expansion age* is ~ 6 M yr.

(ii) The observed velocity gradients along the tails of the globules suggest a *stretching age* for the tails of ~ 3 M yr.

We now wish to discuss several scenarios that may have a bearing on the above two results. The rough agreement between the expansion age and the ages of the tails suggests that both the formation of the tails and the expansion of the globules may be due to a common cause. The presence of young stars in this region with estimated ages ranging from 10^5 to a few 10^6 years is an important clue. Some of these are embedded in the heads of the CGs, while others are isolated. CG 1 has an embedded star with age $\sim 10^6$ yrs (Brand *et al.* 1983, Reipurth 1983), and the embedded IR source CG 30IRS4 in CG 30 has an age $\sim 10^6$ yrs (Pettersson, 1984). The dynamical ages of the bipolar outflows associated with HH 46–47, HH 120 and HH 56–57 are $\sim 10^5$ yrs (Olberg *et al.* 1988). All these strongly point to the possibility that the processes responsible for the expansion of the globules as well as their cometary appearance have also triggered star

formation in some of them. The various possible mechanisms are (i) supernova explosion(s), (ii) radiation from massive stars found in the central region, and (iii) stellar wind from these massive stars. Before discussing each of these scenarios it would be useful to have an estimate of the kinetic energy of a typical globule and its momentum. Assuming a typical CG mass $\sim 20 M_{\odot}$ (Harju *et al.* 1990; Sridharan 1992) and an expansion velocity of 12 kms^{-1} the kinetics energy is $\sim 3 \times 10^{46}$ ergs per globule and its momentum $\sim 5 \times 10^{40}$ gm cms^{-1} We now proceed to make simple estimates for energy and momentum that can be imparted to globule from each of the processes mentioned above.

8.1 *Supernova Explosion(s)*

According to prevalent opinion the Gum Nebula is an old supernova remnant with an age $\sim 10^6$ yrs (Reynolds 1976; Leahy, Nousek & Garmire 1992). Therefore it is natural to ask if the original explosion that created the Gum Nebula could itself be responsible for the observed properties of the system of CGs. Assuming an ejected mass of $8M_{\odot}$, and an energy of explosion 5×10^{51} ergs and a typical CG size of 0.5 pc, we estimate that a typical CG has to be not more than a few pc from the explosion center in order to intercept sufficient momentum. This is a plausible scenario but it should be pointed out that the center of the Gum Nebula shell is 4.5° north of the *center* derived from the tail directions of the CGs. However, we would not like to over-stress this point because of the inherent difficulties in determining the center of explosion of such an old SNR. A more serious difficulty is the following: Although the original explosion could have caused the expansion of the system of CGs and the observed tail structures, the presently observed ionised bright rims cannot be attributed to it, as argued before in section 3 in a similar context.

8.2 *Radiation Pressure*

The most massive star in the region is ζ Pup (O4f) and therefore is the most significant source of photons for exerting radiation pressure. Its luminosity is 9×10^5 $L_{\odot}$ (Bohannan *et al.* 1986). The CG closest to ζ Pup is at a distance of 40 pc from it. For a typical CG size of 0.5 pc, we estimate that over 6 million years (the expansion age) the total kinetic energy and momentum acquired by a CG would be 3×10^{48} ergs and 10^{38} gmcms^{-1}, respectively. Even if we assume that the CG was much bigger to start with, and include the radiation from the other stars as well, the momentum imparted will fall short of the required 5×10^{40} gm cms^{-1}. In this estimate we have assumed 100% efficiency of momentum transfer from the photons to the CG. We therefore conclude that radiation pressure cannot be the sole cause for the expansion of the system.

8.3 *Stellar Wind*

Both Wolf-Rayet stars and O type giants are known to have strong stellar winds reaching terminal velocities upto 3000 kms^{-1} with mass loss rates as high as 10^{-5}

$M_\odot\,yr^{-1}$. The stellar wind from ζ Pup has a velocity of 2600 kms^{-1} and the mass loss rate is $5 \times 10^{-6} M_\odot\,yr^{-1}$ (Bohannan *et al.* 1986). We estimate the energy and momentum intercepted to be 6×10^{47} ergs and $10^{38}\,gm\,cms^{-1}$, respectively, over 6 million years. Stellar wind from γ^2 Vel will merely double these numbers and the momentum available will be less by an order of magnitude even given the assumed 100% efficiency of conversion of the stellar wind momentum to cloud momentum.

8.4 *Rocket Effect*

Finally, we consider the rocket effect resulting from the anisotropic expansion of the hot ionised gas from the bright rims first proposed by Oort and Spitzer (1955) for accelerating interstellar clouds. Reipurth (1983) has estimated that ζ Pup alone can easily account for observed ionisation level ($n_e \sim 100\,cm^{-3}$) at the bright rims. Using mass loss rates derived by Reipurth (1983) and an expansion velocity of the hot gas of 10 kms^{-1} (velocity of sound in the bright rim) we estimate the total momentum acquired by a typical globule due to the rocket effect operating for 6 million years to be $\sim 10^{42}\,gm\,cms^{-1}$ the required momentum being $\sim 5 \times 10^{40}\,gm\,cms^{-1}$. If we include γ^2 Vel and the other B stars, the clouds can be easily accelerated to the observed velocities even with larger initial masses. From the above discussion it appears that the only plausible mechanism which can explain both the bright rims and the expansion velocities is the heating caused by radiation (and possibly stellar wind) from the stars in the central region and the consequent rocket effect. In this paper we do not intend to go into the details of the energetics or the mechanism of formation of the tails. This we propose to do in a subsequent paper. We mention in passing that Bertoldi and McKee (1990) have shown that UV radiation and stellar wind can result in molecular clouds developing tail-like structures.

If one accepts this scenario, viz, that the expansion of the system and all the other features of the CGs are due to the luminous stars in the region, then one has to explain why there is a common *center of expansion.* This is because the sources causing the rocket effect are distributed around the *center.* This suggests that the center of expansion may be associated with event(s) which may have triggered the formation of the massive stars themselves.

9. Summary

We shall now summarize our main findings. Our objective was to study the kinematics of the system of cometary globules in the Gum Nebula. Towards this aim, we measured the radial velocities of 38 globules using the $J = 1 \rightarrow 0$ line of ^{12}CO. In addition we measured the radial velocities at a few points along the tails for 21 globules. This was done to study gas motions in the tails. As argued in section 5, our observations clearly show that the kinematics of the CGs cannot be interpreted in terms of a model where galactic rotation effects dominate, as was claimed by Z83 based on their study of a smaller sample of CGs. Our study points to two clear interpretations:

1. The distribution of the radial velocities of the heads of the cometary globules, after galactic differential rotation is subtracted, is best understood in terms of an

expansion of the system about a common *center*. The data is better fit by a model in which the globules are non-uniformly distributed throughout the interior of a sphere, rather than in a shell. The expansion velocity of the outermost globules is $\sim 12\,\mathrm{kms}^{-1}$. The implied *expansion age* of the system is ~ 6 M yr.

2. Some of the cometary tails show systematic velocity gradients. It is interesting that the estimated age for the formation of the tails inferred from these velocity gradients is about the same (~ 3 M yr) as the expansion age.

The presence of young stars with ages $\sim 10^5$–10^6 yr embedded in the heads of some of the globules suggests that their formation was triggered by the same mechanism responsible for the expansion and the formation of the tails. Regarding the underlying mechanism, whereas the supernova explosion whose remnant is the Gum Nebula might have had an important influence on the dynamics of the system of globules, it is extremely unlikely that the bright ionised rims of the CGs can be understood in terms of an event that occurred $\sim 10^6$ yr ago. In our opinion, the origin of the motions is due to a *rocket effect* resulting from an anisotropic evaporation of gas as envisaged a long time ago by Oort & Spitzer (1955). The most likely cause for this is the UV radiation from ζ Pup, γ^2 Vel and the other early type stars in the central region.

Acknowledgements

I wish to express my sincere thanks to the members of the Millimeter-wave Laboratory and the Observatory staff of the Raman Research Institute for their enthusiastic help and support over the years. It gives me great pleasure to thank B. Ramesh, V. Radhakrishnan and G. Srinivasan for encouragement and numerous discussions, as well as for critical comments which significantly improved the manuscript. My thanks are also due to C. S. Shukre and D. Bhattacharya for their comments on the manuscript. I am grateful to an anonymous referee for pointing out an error in equation 2 in an earlier version of the paper and for suggestions to shorten the paper.

References

Bally, J., Langer, W. D., Wilson, R. W., Stark, A. A., Pound, M. W. 1991, preprint.
Bertoldi, F., McKee, C. F. 1990, *Astrophys. J.*, **354**, 529.
Block, D. L. 1990, *Nature*, **347**, 452.
Bohannan, B., Abbot, D. C., Voels, S. A., Hummer, D. G. 1986, *Astrophys. J.*, **308**, 728.
Bok, B. 1978, *Publ. astr. Soc. Pacific*, **90**, 489.
Brand, P. W. J. L., Hawarden, T. G., Longmore, A. J., Williams, P. M., Caldwell, J. A. R. 1983, *Mon. Not. R. astr. Soc.*, **203**, 215.
Brandt, J. C., Stecher, T. P., Crawford, D. L., Maran, S. P. 1971, *Astrophys. J. (Letters)*, **163**, L99.
Bruhweiler, F. C. 1983, *Comments Astrophys.*, **10**, 1.
Caswell, J. L., Lerche, I. 1979, *Mon. Not. R. astr. Soc.*, **187**, 201.
Cernicharo, J., Bachiller, R., Duvert, G., Gonzalez-Alfonso, E., Gomez-Gonzalez, J. 1991, *Astr. Astrophys.*, accepted.
Claria, J. J. 1982, *Astr. Astrophys. Suppl.*, **47**, 323.
Dibai, E. A. 1963, *Soviet Astr.-AJ*, **7**, 606.
Dubner, G. M., Arnal, E. M. 1988, *Astr. Astrophys. Suppl.*, **75**, 363.
Duvert, G., Cernicharo, J., Bachiller, R., Gomez-Gonzalez, J. 1990, *Astr. Astrophys.*, **233**, 190.
Eggen, O. J. 1980, *Astrophys. J.*, **238**, 627.

Goss, W. M., Manchester, R. N., Brooks, J. W., Sinclair, M. W., Mansfield, G. A., Danziger, I. J. 1980, *Mon. Not. R. astr. Soc.*, **191**, 537.
Graham, J. A. 1986, *Astrophys. J.*, **302**, 352.
Graham, J. A., Heyer, M. H. 1989, *Publ. astr. Soc. Pacific*, **101**, 573.
Green, D. A. 1984, *Mon. Not. R. astr. Soc.*, **209**, 449.
Gum, C. S. 1952, *Observatory*, **72**, 151.
Gum, C. S. 1955, *Mem. R. astr. Soc.*, **47**, 155.
Harju, J., Sahu, M., Henkel, C., Wilson, T. L., Sahu, K. C., Pottasch, S. R. 1990, *Astr. Astrophys.*, **233**, 197.
Hawarden, T. G., Brand, P. W. J. L. 1976, *Mon. Not. R. astr. Soc.*, **175**, 19P.
Kerr, F. J., Lynden-Bell. D. 1986, *Mon. Not. R. astr. Soc.*, **221**, 1023.
Leahy, D. A., Nousek, J., Garmire, G. 1992, *Astrophys. J.*, **385**, 561.
May, J., Murphy, D. C., Thaddeus, P. 1988, *Astr. Astrophys. Suppl.*, **73**, 51.
Milne, D. K. 1979, *Austr. J. Phys.*, **32**, 83.
Murphy, D. C. 1985, Ph.D. Thesis, Massachusetts Institute of Technology.
Olberg, M., Reipurth, B., Booth, R. S. 1988, in *Symposium on Physics and Chemistry of Interstellar Molecular Clouds: mm and Sub-mm Observations in Astrophysics.* Eds G. Winnewisser & J. T. Armstrong, (Heidelberg: Springer Verlag), p. 120.
Oort, J. H., Spitzer, L. 1955, *Astrophys. J.*, **121**, 6.
Patel, N. A. 1990, Ph.D. Thesis, Indian Institute of Science, Bangalore.
Pettersson, B. 1984, *Astr. Astrophys.*, **139**, 135.
Pettersson, B. 1987, *Astr. Astrophys.*, **171**, 101.
Pettersson, B. 1991, in *Low Mass Star Formation in Southern Molecular Clouds*, Ed. B. Reipurth, ESO Scientific Report No. 11, p. 69.
Reipurth, B. 1983, *Astr. Astrophys.*, **117**, 183.
Reynolds, R. J. 1976, *Astrophys. J.*, **206**, 679.
Sahu, M., Pottasch, S. R., Sahu, K. C., Wesselius, P. R., Desai, J. N. 1988, *Astr. Astrophys.*, **195**, 269.
Sandford, M. T., Whitaker, R. W., Klein, R. I. 1982, *Ap. J.*, **260**, 183.
Sandqvist, Aa. 1976, *Mon. Not. R. astr. Soc.*, **177**, 69P.
Schwartz, R. D. 1977, *Astrophys. J.* (*Letters*), **212**, L25.
Sridharan, T. K. 1992, in preparation.
Srinivasan, G., Dwarakanath, K. S. 1982, *J. Astrophys. Astr.* **3**, 351.
Srinivasan, M., Pottasch, S. R., Sahu, K. C., Pecker, J. -C. 1987, ESO Messenger, No. 51, 11.
Sugitani, K., Fukui, Y., Mizuno, A., Ohashi, N. 1989, *Astrophys. J.* (*Letters*), **342**, L87.
Sugitani, K., Fukui, Y., Ogura, K. 1991, *Astrophys. J. Suppl.*, **77**, 59.
Wallerstein, G., Silk, J., Jenkins, E. B. 1980, *Astrophys. J.*, **240**, 834.
Winkler, P. F., Tuttle, J. H., Kirshner, R. P., Irwin, M. J. 1988, in *Supernova Remnants and the Interstellar Medium*, Eds R. S. Roger & T. L. Landecker, (Cambridge: Cambridge University Press), p. 65.
Woodward, R. P. 1976, *Astrophys. J.*, **207**, 484.
Woodward, R. P. 1979, in *Large Scale Characteristics of the Galaxy, IAU Symp.* **84**, Ed W. B. Burton, (Reidel, Dordrecht, Holland), p. 159.
Zarnecki, J. C., Culhane, J. L., Toor, A., Seward, F. D., Charles, P. A. 1978, *Astrophys. J.* (*Letters*), **219**, L17.
Zealey, W. J., Ninkov, Z., Rice, E., Hartley, M., Tritton, S. B. 1983, *Astrophys. Letters*, **23**, 119. (Z83).